

**Supporting information for:**

**Fates of secondary organic aerosols in the atmosphere identified from compound-specific dual-carbon isotope analysis of oxalic acid**

Buqing Xu<sup>1,2</sup>, Jiao Tang<sup>1,2</sup>, Tiangang Tang<sup>1,3</sup>, Shizhen Zhao<sup>1,2</sup>, Guangcai Zhong<sup>1,2</sup>, Sanyuan Zhu<sup>1,2</sup>, Jun Li<sup>1,2</sup>, Gan Zhang<sup>1,2\*</sup>

<sup>1</sup>State Key Laboratory of Organic Geochemistry, Guangzhou Institute of Geochemistry, Chinese Academy of Sciences, Guangzhou 510640, China.

<sup>2</sup>CAS Center for Excellence in Deep Earth Science, Guangzhou 510640, China

<sup>3</sup> Key Laboratory of Agro-ecological Processes in Subtropical Region, Institute of Subtropical Agriculture, Chinese Academy of Sciences, Changsha, 410125, China.

\*Correspondence: Gan Zhang ([zhanggan@gig.ac.cn](mailto:zhanggan@gig.ac.cn))

**This PDF file includes:**

**1. Supplementary Figure (Figure 1–4)**

**2. Supplementary Table (Table 1–5)**

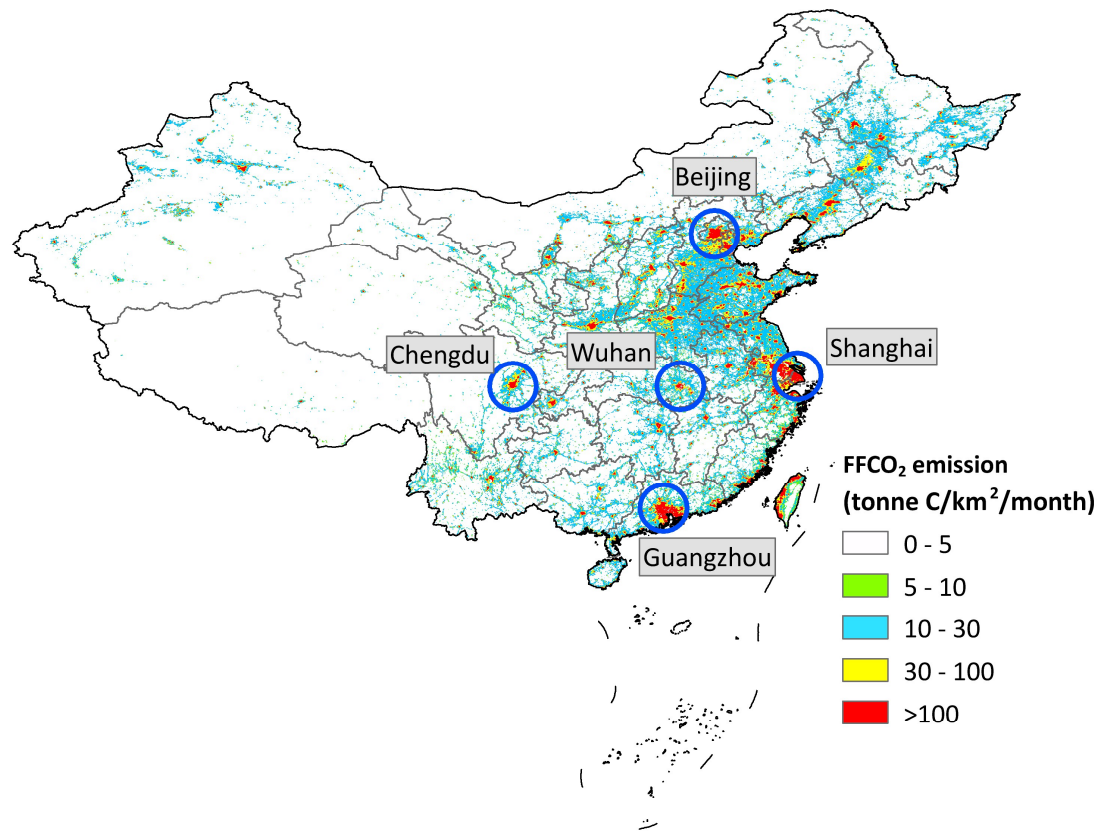


**Figure S1.** Locations of the five megacities (Beijing, Chengdu, Guangzhou, Shanghai, and Wuhan) and average fossil fuel CO<sub>2</sub> (FF CO<sub>2</sub>) emissions during the year 2018. FF CO<sub>2</sub> emissions indicating high levels of anthropogenic activities over the five megacities. The FF CO<sub>2</sub> emission data is obtained from Open-source Data Inventory for Anthropogenic CO<sub>2</sub> ([https://db.cger.nies.go.jp/dataset/ODIAC/DL\\_odiac2020b.html](https://db.cger.nies.go.jp/dataset/ODIAC/DL_odiac2020b.html)). The administration boundaries in the map are originated from map products of National Geomatics Center of China (<https://www.webmap.cn/>).

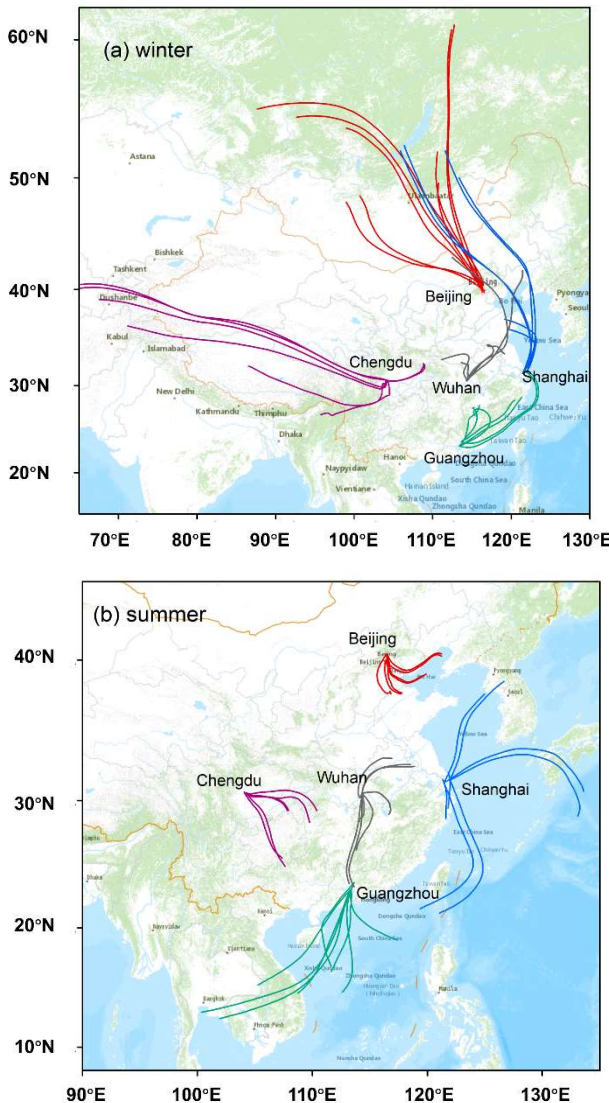


**Figure S2.** Cluster analysis of 3-day air mass backward trajectories computed at an altitude of 100 m for the sampling sites in Beijing, Shanghai, Guangzhou, Wuhan, and Chengdu during January 2018 (a) and July 2018 (b). The maps are originated from ArcGIS hub free map data (<https://hub.arcgis.com/maps/0c539fdb47d34b17bd1452f6b9f49e97/explore?location=17.762116%2C-74.005269%2C3.65>).

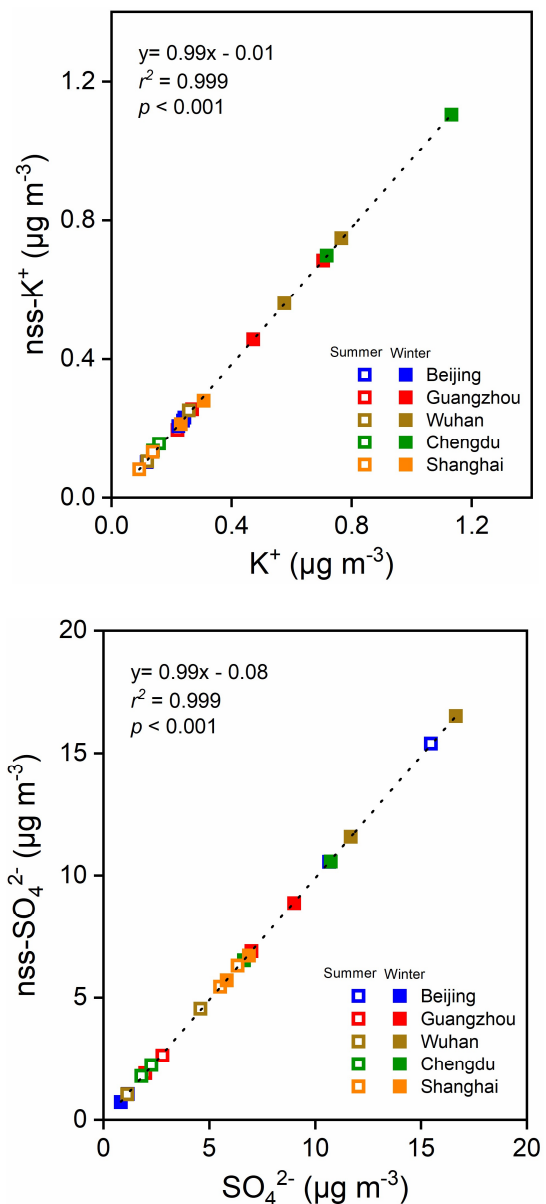


**Figure S3.** Ratios of non-sea-salt potassium (nss-K<sup>+</sup>) to total K<sup>+</sup> and non-sea-salt sulfate (nss-SO<sub>4</sub><sup>2-</sup>) to total SO<sub>4</sub><sup>2-</sup>.

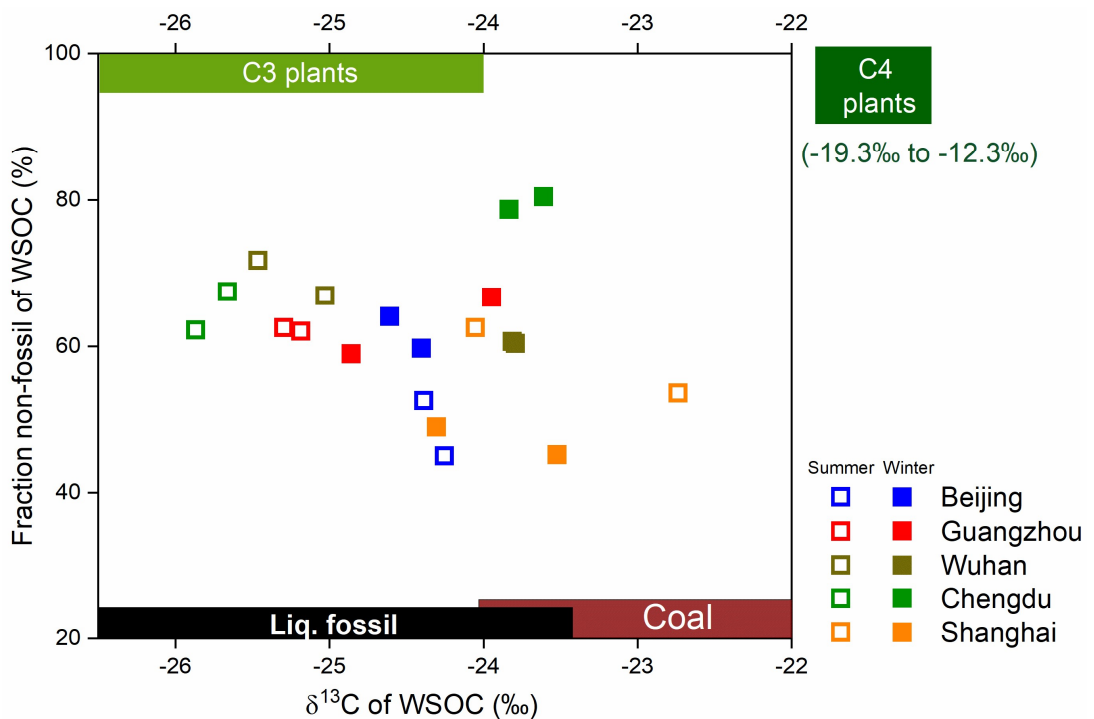


**Figure S4.**  $^{14}\text{C}$ -based non-fossil source fractions plotted against the  $\delta^{13}\text{C}$  values for water-soluble organic carbon (WSOC) in  $\text{PM}_{2.5}$  collected in Beijing (blue), Guangzhou (red), Wuhan (brown), Chengdu (green), and Shanghai (orange) in summer (open squares) and winter (filled squares).

**Table S1.** Information on sampling sites and deployment periods.

City	Site attribution	Location	Cycle starts	Cycle ends	Cycle starts	Cycle ends
			in winter	in winter	in summer	in summer
Beijing	Urban	39.974°N, 116.370°E	2018/1/5	2018/1/12	2018/7/28	2018/8/3
	Suburban	40.408°N, 116.674°E	2018/1/5	2018/1/12	2018/7/28	2018/8/3
Shanghai	Urban	31.316°N, 121.423°E	2018/1/19	2018/1/25	2018/7/28	2018/8/3
	Suburban	31.524°N, 121.959°E	2018/1/18	2018/1/24	2018/7/28	2018/8/3
Guangzhou	Urban	23.149°N, 113.358°E	2018/1/18	2018/1/24	2018/6/29	2018/7/5
	Suburban	23.650°N, 113.624°E	2018/1/18	2018/1/24	2018/6/29	2018/7/5
Wuhan	Urban	30.531°N, 114.308°E	2018/1/19	2018/1/25	2018/7/28	2018/8/3
	Suburban	30.531°N, 114.332°E	2018/1/18	2018/1/24	2018/7/28	2018/8/3
Chengdu	Urban	30.629°N, 104.064°E	2018/1/18	2018/1/24	2018/7/28	2018/8/3
	Suburban	30.563°N, 104.272°E	2018/1/18	2018/1/24	2018/7/28	2018/8/3

**Table S2.** Mass concentration of dicarboxylic acids, oxocarboxylic acids, and  $\alpha$ -dicarbonyls in PM<sub>2.5</sub> samples from the five hot spot emission locations of China.

	Summer (N = 10)		Winter (N = 10)	
	Range	Mean/SD	Range	Mean/SD
<b>I. Dicarboxylic Acids, ng m<sup>-3</sup></b>				
Oxalic, C <sub>2</sub>	59.2-713.3	412.8±201.5	19.2-1077.9	740.1±324.4
Malonic, C <sub>3</sub>	3.1-44.7	30.5±12.2	0.8-53	26.8±16
Succinic, C <sub>4</sub>	3.1-44.5	25.4±11.9	1.6-66	39.5±21.3
Glutaric, C <sub>5</sub>	0.6-9.7	4.9±2.7	0.3-18.9	10.7±6
Adipic, C <sub>6</sub>	0.5-5	2.9±1.5	0.2-8.7	4.8±2.5
Pimelic, C <sub>7</sub>	0.2-2.5	1.3±0.8	0-5.2	2.3±1.5
Suberic, C <sub>8</sub>	0.4-5.2	2.6±1.6	0.1-7.7	3.2±2.2
Azelaic, C <sub>9</sub>	0.7-31.3	11.4±9	0.3-21.4	8.6±6.2
Sebacic, C <sub>10</sub>	0.1-1.6	0.8±0.4	0-3.3	1.3±1.1
Undecanedioic, C <sub>11</sub>	0.1-1.9	0.6±0.5	0-1.9	0.7±0.6
Dodecanedioic, C <sub>12</sub>	0-0.4	0.2±0.1	0-0.7	0.3±0.2
Methylmalonic, iC <sub>4</sub>	0.1-0.9	0.7±0.3	0-1.1	0.6±0.3
Methylsuccinic, iC <sub>5</sub>	0.3-2.7	1.8±0.8	0.3-7.1	4.1±2.5
2-Methylglutaric, iC <sub>6</sub>	0.1-0.9	0.5±0.3	0.1-1.7	1±0.6
Maleic, M	0.2-3.8	1.5±1	0.1-4.1	2±1.2
Fumaric, F	0.2-1.7	1±0.4	0.1-1.5	0.8±0.4
Methylmaleic, Mm	0.4-4	2.9±1.2	0.3-7.6	3.7±2
Phthalic, Ph	2.1-25.4	10.2±7.1	1.3-17.7	6±5
Isophthalic, iph	0-0.4	0.2±0.1	0-0.7	0.2±0.2
Terephthalic, tPh	0.6-11.2	5.7±4	0.4-18.1	6.6±5.6
4-Ketopimelic, kC <sub>7</sub>	0.2-8.5	4±2.6	0-6.7	1.9±2
Total diacids	75.5-871	521.8±233.8	25.4-1269.2	865.2±384.5
<b>II. Oxocarboxylic Acids, ng m<sup>-3</sup></b>				
Pyruvic, Pyr	0.4-10	6.4±2.8	0.2-23.4	9.3±7.3
Glyoxylic, $\omega$ C <sub>2</sub>	2.5-27.1	18.2±7.4	2.1-69.3	41.1±20.8
3-Oxopropanoic, $\omega$ C <sub>3</sub>	0.5-5.1	3.4±1.4	0.4-2.7	1.6±0.7
4-Oxobutaboic, $\omega$ C <sub>4</sub>	0.5-5.6	3.6±1.6	0.4-4.4	2.1±1.1
5-Oxopentanoic, $\omega$ C <sub>5</sub>	0-11.9	1.9±3.8	0-29.7	14.9±10.6
6-Oxoheptanoic, $\omega$ C <sub>6</sub>	0-4.6	2.5±1.4	0-5.5	3.1±1.9
Total oxoacids	3.9-55.9	36±15.1	3.1-113.1	72±37.9
<b>III. <math>\alpha</math>-Dicarbonyls, ng m<sup>-3</sup></b>				
Glyoxal, Gly	0.1-15.2	3.7±5	0.1-27	7.7±8.4
Methylglyoxal, mGly	11.2-72.2	33.3±20.8	12.2-89.7	56.6±28.7
Total dicarbonyls	11.2-87.4	37±25.5	12.3-111.1	64.3±35.8

**Table S3.** The mass concentration, stable carbon composition ( $\delta^{13}\text{C}$ , ‰), and  $^{14}\text{C}$ -based source apportionment (fraction of non-fossil;  $f_{NF}$ ) of oxalic acid in the PM<sub>2.5</sub> samples from the five hot spot emission locations of China.

City	Season	Site attribute	Concentration (ng m <sup>-3</sup> )	$\delta^{13}\text{C}$ (‰)	$f_{NF}$ (%)
Guangzhou	Summer	Suburban	491.3	-22.8±0.5	75.7±1.7
		Urban	502.0	-23.2±0.2	72.7±2.4
	Winter	Suburban	888.4	-26.7±0.6	63.6±1.2
		Urban	571.2	-27.5±0.4	63.7±1.5
Beijing	Summer	Suburban	705.0	-22±1.0	57.5±1.4
		Urban	713.3	-23.7±0.1	43.5±1.3
	Winter	Suburban	19.2	-22±1.1	nd
		Urban	424.5	-29.7±1.4	44.1±4.9
Wuhan	Summer	Suburban	59.2	-22.3±0.1	nd
		Urban	302.1	-22.6±0.2	73.1±4.4
	Winter	Suburban	732.4	-27±0.4	64.6±1.4
		Urban	1077.9	-27.2±0.6	59.6±1.4
Chengdu	Summer	Suburban	262.7	-23.5±0.6	71.4±5.0
		Urban	316.8	-25.1±0.9	62.8±4.5
	Winter	Suburban	1038.6	-26.9±0.7	63.1±1.3
		Urban	972.1	-26.6±1.2	59.3±1.0
Shanghai	Summer	Suburban	335.5	-14.1±0.1	66±1.8
		Urban	439.6	-18.6±0.2	71.6±1.6
	Winter	Suburban	817.0	-23.7±0.1	41.5±0.5
		Urban	859.5	-24.7±1.0	39.6±1.2

<sup>a</sup> nd: non data

**Table S4.** Compound-specific stable carbon isotope ratios ( $\delta^{13}\text{C}$ , ‰) of dicarboxylic acid and oxocarboxylic acid in PM<sub>2.5</sub> samples from the five hot spot emission locations of China.

	Summer (N = 10)		Winter (N=10)	
	Range	Mean/SD	Range	Mean/SD
<b>I. Dicarboxylic Acids</b>				
Oxalic, C <sub>2</sub>	-25.1 to -14.1	-21.8±3.2	-29.7 to -22.0	-26.2±2.2
Malonic, C <sub>3</sub>	-24.9 to -18.4	-21.7±1.8	-26.7 to -20.7	-23.2±2.1
Succinic, C <sub>4</sub>	-28.6 to -20.7	-24.4±2.1	-27.6 to -23.0	-24.2±1.5
Azelaic, C <sub>9</sub>	-29.8 to -26.7	-28.1±0.8	-32.5 to -26.2	-29±1.7
Phthalic, Ph	-31.7 to -27.8	-29.4±1.3	-37.1 to -26.0	-30.5±3.5
<b>II. Oxocarboxylic Acid</b>				
Glyoxylic, $\omega\text{C}2$	-39.8 to -19.3	-32.5±5.4	-45.9 to -30.1	-37.2±4.9

**Table S5.** The concentrations of major chemical components in PM<sub>2.5</sub> samples from the five hot spot emission locations of China.

	Summer (N = 10)		Winter (N = 10)	
	Range	Mean/SD	Range	Mean/SD
PM <sub>2.5</sub> , $\mu\text{g m}^{-3}$	32.2-163.7	80.5±44.3	2.4-137.8	92.2±44.7
WSOC, $\mu\text{g m}^{-3}$	1.1-3.8	2.2±0.8	1.1-9.6	4.1±2.5
NO <sub>3</sub> <sup>-</sup> , $\mu\text{g m}^{-3}$	0.9-7.9	3.2±2.5	1.4-62.7	26.3±20.1
nss-SO <sub>4</sub> <sup>2-</sup> , $\mu\text{g m}^{-3}$	1.1-15.5	5.3±4.6	0.8-16.6	7.6±4.7
NH <sub>4</sub> <sup>+</sup> , $\mu\text{g m}^{-3}$	0.5-8.2	3.0±2.8	0.7-16.9	7.6±5.2
nss-K <sup>+</sup> , $\mu\text{g m}^{-3}$	0.1-0.3	0.2±0.1	0.1-1.1	0.5±0.3
WSIC <sub>anth</sub> <sup>a</sup> , $\mu\text{g m}^{-3}$	2.5-31.5	11.7±9.6	3.5-100.4	43.5±30.9
ALWC <sup>b</sup> , $\mu\text{g m}^{-3}$	2.6-19.4	8.5±5.1	1.4-229.8	59.7±76.1

<sup>a</sup> anthropogenic water-soluble inorganic constituents (WSIC<sub>anth</sub>) = non-sea-salt (nss) K<sup>+</sup> + nss-SO<sub>4</sub><sup>2-</sup> + NH<sub>4</sub><sup>+</sup> + NO<sub>3</sub><sup>-</sup> + nss-Cl<sup>-</sup> <sup>b</sup> aerosol liquid water content